A Novel Method of Flight Target Altitude Attributes Identification for HFSWR

Shuai Shao, Changjun Yu(✉), and Kongrui Zhao

School of Information and Electrical Engineering,
Harbin Institute of Technology, Weihai 264209, China
yuchangjun@hit.edu.cn

Abstract. Recently, flight target altitude estimation using high frequency surface wave radar (HFSWR) gains popularity. In practical flight target early warning applications, the most concerned characteristics of the targets are generally the high/low altitude attribute and the line-of-sight/over-the-horizon. For HFSWR, the target altitude attribute identification is somewhat more meaningful and available than the accurate altitude estimation. In this paper, a novel method, which is based on the propagation attenuation of the vertically polarized wave at different altitude intervals, is proposed to identify target altitude attribute in HFSWR. The method continuously identify the target altitude attributes and evaluate the credibility of altitude attributes identification. Practical trials demonstrate that the flight target altitude attribute is quickly identified using a small amount of data, and meanwhile the credibility is superior to 0.9.

Keywords: High frequency surface wave radar
Altitude attribute identification · Propagation attenuation

1 Introduction

High frequency surface wave radar (HFSWR), which transmits vertical polarized radio waves along the sea surface, is able to detect flight targets for hundreds of kilometers away [1–4]. The radar has been applied by the maritime surveillance departments to combat sea smuggling, to control maritime traffic and to protect exclusive economic zone [5–7]. HFSWR takes the advantage of the diffraction propagation of the radio wave to detect the over-the-horizon flight targets, while the radar can also be employed to detect the high-altitude line-of-sight target due to the relatively wide vertical beam. However, the signal and data processing methods utilized in traditional HFSWR provide only the distance, velocity and orientation information of the targets, i.e. the altitude information of the flight target is unavailable. Therefore, HFSWR is fails to identify the target altitude attribute, and unable to judge whether it is a high altitude target or a low altitude target. As pointed out in [8], HFSWR cannot immediately distinguish between targets that are at different altitude in the same range over the horizon.

In order to identify the high/low altitude attribute of the flight target, the target altitude can be accurately estimated by the traditional method. However, HFSWR is currently using slope and azimuth information to estimate the altitude of high-altitude

X. Gu et al. (Eds.): MLICOM 2017, Part II, LNICST 227, pp. 351–360, 2018.
https://doi.org/10.1007/978-3-319-73447-7_39

targets, these methods cannot be applied to low-altitude flight target altitude estimates. In [9], a real-time estimation method of altitude and radar cross section (RCS) of target using echo is proposed. However, this method is a multi-solution problem at altitude estimation resulting in highly estimated error and low credibility. Although many improved algorithms are proposed based on the above methods, there is still no fundamental solution to the highly estimated multiresolution problem [10–12] and cannot be applied to HFSWR practical systems so far. From the point of view of engineering application, HFSWR flight target altitude estimation is still in the exploratory stage. In the HFSWR marine flight target early warning applications, whether the target is a high/low altitude flight and line-of-sight/over-the-horizon is mostly concerned. It is more practical to quickly and directly identify the flight target as a high/low altitude attribute, line-of-sight/over-the-horizon attribute, that is to obtain the flight target altitude attribute more than the specific flight altitude of the accurate estimation, and it is easier to realize on the actual HFSWR system.

Based on the above engineering design, this paper focuses on solving the HFSWR flight target high/low altitude attribute, line-of-sight/over-the-horizon attribute identification issue. According to the different propagation attenuation characteristics of the vertically polarized waves in the range of high and low altitude that will be introduced in Sect. 2, a target altitude attribute identification algorithm is proposed without estimating the specific flight altitude of the target in Sect. 3. This method is able to identify the target altitude attribute, and calculate the credibility of altitude attribute identification. Furthermore, in Sect. 4, the algorithm is verified by the in situ data. A brief conclusion is given in Sect. 5.

2 HFSWR Propagation Attenuation

According to the monostatic HFSWR equation, the power of the received signal can be expressed as

$$P_r = P_t G_t \frac{1}{l_b^2(R,h)} \frac{\sigma}{(\lambda^2/4\pi)} G_r \tag{1}$$

where P_r is the received target echo; P_t is the transmitting station signal transmission power; G_t is the transmit antenna gain; G_r is the receive antenna gain; σ is the target RCS; h is the target altitude; R is the distance between the target and the radar observation station; $l_b(\bullet)$ is the surface wave propagation attenuation used by the International Telecommunication Union (ITU), which is a function of the target flight altitude h and the distance R from the target to the observation station; λ is operating wavelength of radar.

The HFSWR Eq. (1) takes the logarithm, and decibel representation is

$$P_r(dB) = -20\lg l_b(R,h) + 10\lg\sigma + 10\lg c \tag{2}$$

where $C = 10\lg c$, $\zeta_b(R,h) = 10\lg l_b(R,h)$ and $\Psi = 10\lg\sigma$. Hence (2) can be expressed as

$$P_r(dB) = -2\zeta_b(R, h) + \Psi + C \quad (3)$$

In (3), it is assumed that the radar system parameters are constant, and C is also known. The target echo is regarded as a known constant, and the target RCS and the wave propagation attenuation have a linear constraint relationship. In addition, the wave propagation attenuation is a function of the target distance and flight altitude. Therefore, to achieve the target flight altitude attribute identification, it is necessary to analyze the propagation attenuation of the vertically polarized wave propagating at different altitude.

In the high frequency band, the Rotheram model takes into account the atmospheric refraction index and expatiates the propagation decay model in detail. The propagation decay curve is adopted by the ITU as radio wave propagation attenuation standard in 10 kHz–30 MHz [13, 14]. Therefore, based on the unique advantage of the Rotheram propagation attenuation model, the Rotheram propagation attenuation model is used to calculate propagation decay curves at different altitude and distances.

For radar operates in 11.2 MHz, the altitude of transmitting station is 20 m, and the range of distance between radar station and target is 30 km–140 km, the low- and high-altitude propagation decay curve is shown in Figs. 1 and 2, respectively. As shown in Fig. 1, the attenuation decreases gradually with the increasing altitude in the low altitude region. When the flight altitude is lower than 2 km, the attenuation at different altitude is different, and the altitude change 0.5 km can cause the deviation of 2 dB. In Fig. 2, the propagation attenuation difference at different altitude is getting less. It can be seen that the difference in propagation attenuation in the high-altitude region is not obvious. Therefore, the different propagation attenuation of the vertical polarization wave propagation attenuation in the different space regions provides the possibility of identifying the target altitude attribute.

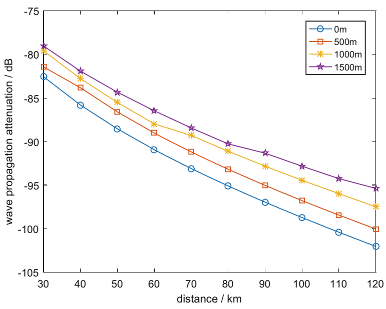

Fig. 1. Low-altitude propagation attenuation

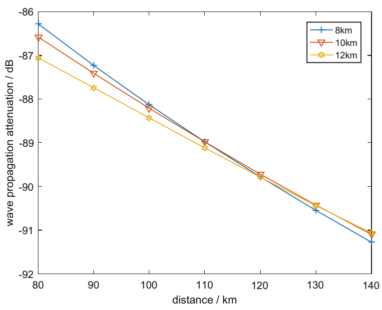

Fig. 2. High-altitude propagation attenuation

3 Altitude Attribute Identification Algorithm

The purpose of this paper is to directly identify the altitude attribute of the flight target without estimating the specific flight target altitude, and to improve the estimating performance of goal threat in HFSWR.

Line-of-sight/over-the-horizon of the target is related to the target distance and flight altitude. In order to simplify line-of-sight/over-the-horizon attribute identification problem complexity, the target high/low altitude flight status is identified before identifying the altitude attribute, then the high/low altitude flight status is used to identify line-of-sight/over-the-horizon attribute of the target. Therefore, the altitude attribute of the flight target is divided into four categories: high-altitude and line-of-sight, high-altitude and over-the-horizon, low-altitude and line-of-sight, low-altitude and over-the-horizon.

In order to make full use of the propagation attenuation characteristics of vertically polarized waves in different altitude intervals, the target echo correction is needed in the altitude attribute identification algorithm.

In the low-altitude region, the attenuation of the surface wave caused by seawater is large. Therefore, it is assumed that the height region of 0–2 km is a low-altitude area. The altitude of the 0–2 km range is divided into four altitude sub-intervals, the altitude division nodes are respectively $h_0 = 0$ km, $h_1 = 0.5$ km, $h_2 = 1$ km, $h_3 = 1.5$ km, $h_4 = 2$ km. The propagation attenuation on the ith altitude sub-interval is approximated by the propagation attenuation on the node altitude h_i. That is

$$\zeta_b(R, h_{i-1} < h < h_i) \approx \zeta_b(R, h_i) \quad i = 1, 2, 3, 4 \tag{4}$$

The target altitude is higher in the high altitude region, and the influence of the flight altitude on the attenuation of the radio wave propagation is very small, and the influence of the altitude on the target echo can be neglected. Thus, the propagation attenuation at the altitude of the $h_H = 10$ km is used instead of the propagation attenuation at any altitude in the high altitude region. That is

$$\zeta_b(R, h) \approx \zeta_b(R, h_H = 10\,\text{km}) \tag{5}$$

Thus, the target echo corresponding to each altitude node is

$$P_r(dB) = -2\zeta_b(R, h_i) + \Psi + C \quad i = 1, 2, 3, 4, H \tag{6}$$

In this paper, we use the multi-model algorithm to first identify the target high/low altitude flight state. Independent filtering models are constructed on each altitude sub-interval of the low altitude region and the high altitude region. In the filtering model of the ith altitude sub-interval, the target state vector is defined as

$$\mathbf{X}_k^i = \left[\Psi_k, \dot{\Psi}_k\right]^T \tag{7}$$

where Ψ_k is the RCS size of the target relative to the station at k, and $\dot{\Psi}$ is the target RCS rate of change at k. It can be seen from (7) that the target state vector does not contain unknown altitude information and contains only RCS information, thus avoiding the multi-solution problem of state estimation. The target state equation of the ith filter model is defined as

$$\mathbf{X}_k^i = \mathbf{F}\mathbf{X}_{k-1}^i + \mathbf{v}_{k-1} \tag{8}$$

where $\mathbf{F} \in \mathbf{R}^{2\times 2}$ is the state transition matrix,$\mathbf{v}_{k-1}$ is the white Gaussian process noise with mean of 0 and variance of $\boldsymbol{Q}_{k-1}^i$.

The target echo is used as the observation value of each filter model, and the observation equation is defined as

$$P_r(dB) = -2\zeta_b(R, h_i) + \Psi_k + C + \omega_k \tag{9}$$

where ω_k is the white Gaussian observation noise with mean of 0 and variance of R_k.

A set of multi-models filters can be established using the filtering model on all altitude sub- intervals of the low-altitude region and the high-altitude region. This set of multi-models filters is defined as follows

$$\begin{cases} \mathbf{X}_k^i = \mathbf{F}\mathbf{X}_{k-1}^i + \mathbf{v}_{k-1} \\ P_r(dB) = -2\zeta_b(R, h_i) + \Psi_k + C + \omega_k \end{cases} \quad i = 1, 2, 3, 4, H \tag{10}$$

In the high/low altitude flight state identification, the Kalman filter algorithm is used to calculate the predicted value $\hat{Z}_{k/k-1}^i$, the state $\hat{X}_{k/k}^i$ and the covariance $P_{k/k}^i$ of the ith filter model at k . $\hat{Z}_{k/k-1}^i$ is used to calculate the confidence level of the high/low altitude flight state. At the time of $k+1$, the ith filter model is initialized with $\hat{X}_{k/k}^i$ and $P_{k/k}^i$. The target high/low altitude flight status identification process is shown in Fig. 3.

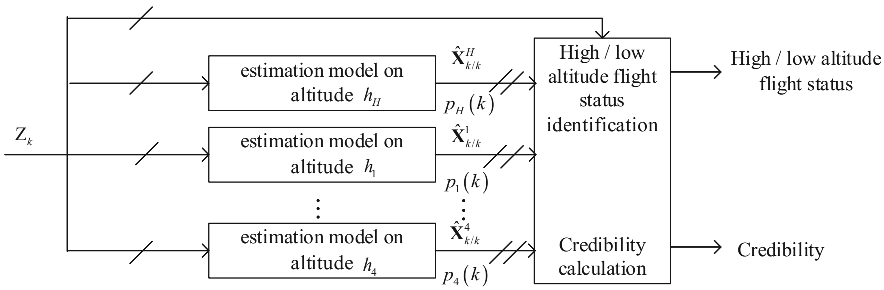

Fig. 3. High/low altitude flight status identification flow chart

The input information Z_k is the target echo value; the model on the altitude h_i is the state filtering model defined by (10). The high/low altitude flight status identification and confidence calculation module input information is estimated value $\hat{X}_{k/k}^i$ of the state filter model and the likelihood function $p_i(k)$ of the filtering model. For the ith filter model, likelihood value of the observed value Z_k is

$$p(Z_k/h_i) = \frac{1}{\sqrt{2\pi|\mathbf{S}_k^i|}} \exp\left\{-\frac{1}{2}\mathbf{\Delta}\hat{Z}^i_{k/k-1}{}^T\mathbf{S}_k^{i-1}\mathbf{\Delta}\hat{Z}^i_{k/k-1}\right\} \tag{11}$$

where $\mathbf{S}_k^i$ is the new covariance matrix of ith filtering model at time k; $\mathbf{\Delta}\hat{Z}^i_{k/k-1}$ is the new information of ith filter model at time k, defined as

$$\mathbf{\Delta}\hat{Z}^i_{k/k-1} = Z_k^i - \hat{Z}^i_{k/k-1} \tag{12}$$

The confidence values of high/low altitude flight states are defined by the likelihood function given by (11) as follows:

(1) High altitude flight state confidence value

$$\begin{aligned} p(D_1(k)) &= p(h_H(k)) \\ &= \frac{p(Z_k/h_H)\cdot p(h_H(k-1))}{p(Z_k/h_H)\cdot p(h_H(k-1)) + \sum_{j=1}^{4} p(Z_k/h_j)\cdot p(h_j(k-1))} \end{aligned} \tag{13}$$

(2) Low altitude flight state confidence value

$$\begin{aligned} p(D_2(k)) &= \max_{i=1,2,3,4}\{p(h_i(k))\} \\ &= \max_{i=1,2,3,4}\left\{\frac{p(Z_k/h_i)\cdot p(h_i(k-1))}{p(Z_k/h_H)\cdot p(h_H(k-1)) + \sum_{j=1}^{4} p(Z_k/h_j)\cdot p(h_j(k-1))}\right\} \end{aligned} \tag{14}$$

If $p(D_1(k)) > p(D_2(k))$, it is identified that the target is a high altitude flight state. Conversely, the target is identified to be low altitude flight state. The high/low altitude flight states of the target can be identified by (13) and (14), but the target flight altitude information is not given directly. However, the high and low altitude flight states of the identification defined by (13) and (14) can indirectly determine the altitude sub-interval of the target.

Therefore, the altitude attribute is defined by the high/low altitude flight state and the line of sight/over-the-horizon, as follows

(1) Assuming $p(D_1(k)) > p(D_2(k))$ and $R(km) < 4.2\sqrt{h_H(m)}$, then the target is the high-altitude line-of-sight attribute
(2) Assuming $p(D_1(k)) > p(D_2(k))$ and $R(km) > 4.2\sqrt{h_H(m)}$, then the target is the high-altitude and over-the-horizon attribute
(3) Assuming $p(D_1(k)) < p(D_2(k))$ and $R(km) < 4.2\sqrt{h_l(m)}$, where $l = \arg\max_{i=1,2,3,4}\{p(h_i(k))\}$, then the target is the low-altitude and line-of-sight attribute

(4) Assuming $p(D_1(k)) < p(D_2(k))$ and $R(km) > 4.2\sqrt{h_l(m)}$, where $l = \arg\max_{i=1,2,3,4} \{p(h_i(k))\}$, then the target is the low-altitude and over-the-horizon attribute.

When the target satisfies the altitude attribute criterion (1) or (2), the altitude attribute credibility value is defined as $p(D_1(k))$ (Fig. 4).

When the target satisfies the altitude attribute criterion (3) or (4), the altitude attribute credibility value is defined as $p(D_2(k))$.

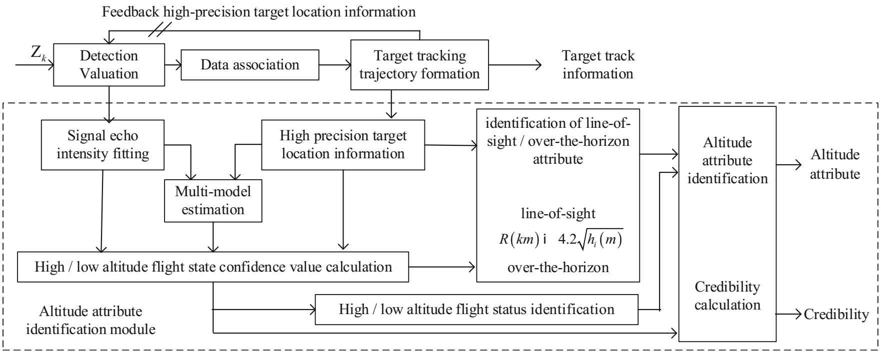

Fig. 4. Frame of flight target altitude attribute identification algorithm for HFSWR

4 Practical Trials Validation

This section uses Weihai high frequency surface wave radar station experimental data to analyze the performance of the altitude attribute identification algorithm. HFSWR operating frequency is 11.2 MHz, the transmission power is 1 kw, the sampling period is 10 s. The target distance observation error is 1 km, and the target echo observation error is 1 dB.

(1) The track of the first batch flight targets is shown in Fig. 5. The target flight height is 200 m, and the azimuth angle of the radar station is 14° and the distance between the target and the observation station is 23.2 km–59.5 km. Figure 6 shows that after four sampling points, the target low altitude flight state reliability value is close to 1, and the high altitude flight state reliability value is close to 0. Therefore, the target can be judged as a low-altitude flight target.

(2) The second batch of aircraft target track is shown in Fig. 7, the aircraft target flight direction suspected of Japan, South Korea direction. Figure 8 shows that the result of the altitude estimation matches with the flight altitude of the international civil aviation aircraft. The target heading speed is 921.6 km/h and also conforms to the international flight speed.

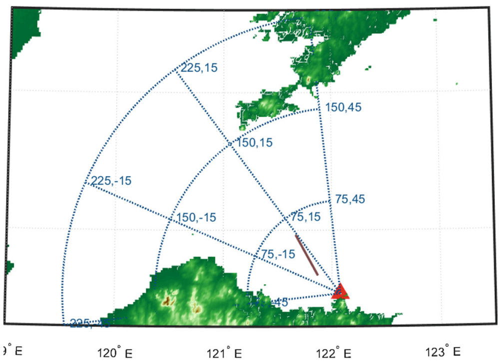

Fig. 5. Target relative to the observation station track

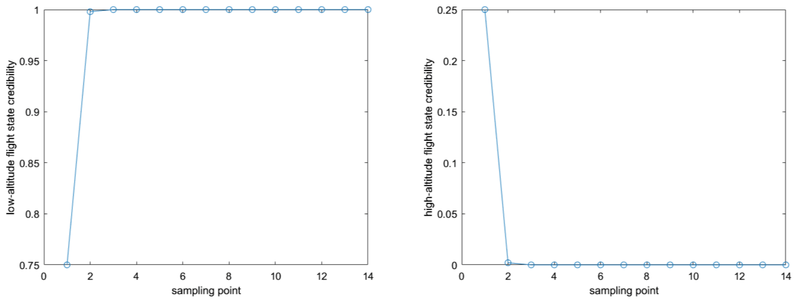

a) low-altitude flight state credibility b) high-altitude flight state credibility

Fig. 6. High/low-altitude flight state credibility

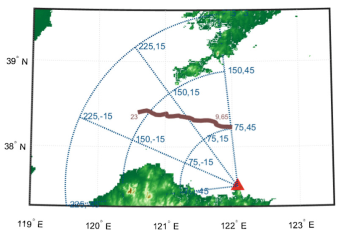

Fig. 7. Target track

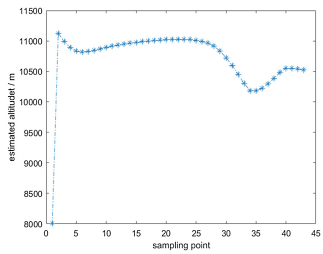

Fig. 8. Estimated altitude results

The high and low altitude flight states values shown in Fig. 9 indicate that the target is at high altitude and the high altitude flight state reliability is more than 0.95. In the calculation of the high-altitude flight state confidence value shown in Fig. 9(a), $p(h_H)$ is more than 0.95. The target is within the high altitude range defined herein, and its

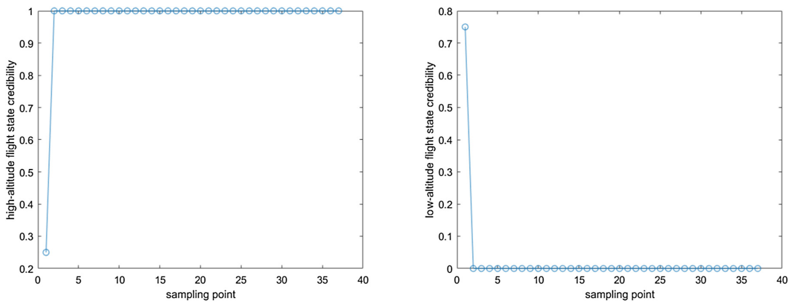

a) high-altitude flight state credibility b) low-altitude flight state credibility

Fig. 9. High/low-altitude flight state credibility

altitude is replaced by h_H = 10 km, and the target distance is about 75 km–160 km. According to the line-of-sight and over-the-horizon attribute judgment criterion, the target distance and the altitude always meet $R(km) < 4.2\sqrt{h_{\mathrm{H}}(m)}$, the target is the line-of-sight target. In summary, the target attribute is the high-altitude line-of-sight attribute. As can be seen from the altitude attribute confidence value, the high-altitude flight state confidence value shown in Fig. 9(a) is also the altitude attribute identification confidence value.

5 Conclusion

Based on the different propagation attenuation characteristics of vertically polarized waves in high-altitude and low-altitude regions, this paper proposed an algorithm of flight target altitude attribute identification and target altitude attribute identification credibility calculation, and defined an altitude attribute identification criteria. The algorithm used the target high/low altitude flight status information and target distance information to determine the target line-of-sight and over-the-horizon attributes. The practical trials showed that the proposed algorithm identified the line-of-sight and over-the-horizon attributes of the flight target, in the meanwhile, identified the high/low altitude flight status of the flight target. The correctness of the target altitude attribute identification is 0.9 or more.

Acknowledgments. The authors would like to thank the support of National Natural Science Foundation projects 61171188 and 61571159 for the project.

References

1. Anderson, S.J.: Optimizing HF radar siting for surveillance and remote sensing in the strait of Malacca. IEEE Trans. Geosci. Remote Sens. **51**(3), 1805–1816 (2013)
2. Xie, J., Sun, M., Ji, Z.: First-order ocean surface cross section for shipborne HFSWR. Electron. Lett. **49**(16), 1025–1026 (2013)

3. Zhou, H., Wen, B., Wu, S.: Ionospheric clutter suppression in HFSWR using multilayer crossed-loop antennas. IEEE Geosci. Remote Sens. Lett. **11**(2), 429–433 (2013)
4. Grosdidier, S., Forget, P., Barbin, Y., et al.: HF bistatic ocean doppler spectra: simulation versus experimentation. IEEE Trans. Geosci. Remote Sens. **52**(4), 2138–2148 (2014)
5. Bruno, L., Braca, P., Horstmann, J., et al.: Experimental evaluation of the range-doppler coupling on HF surface wave radars. IEEE Geosci. Remote Sens. Lett. **10**(4), 850–854 (2013)
6. Sathyan, T., Chin, T.J., Arulampalam, S., et al.: A multiple hypothesis tracker for multitarget tracking with multiple simultaneous measurements. IEEE J. Sel. Topics Signal Process. **7**(3), 448–460 (2013)
7. Abramovich, Y.I., Frazer, G.J., Johnson, B.A.: Principles of mode-selective MIMO OTHR. J. IEEE Trans. Aerosp. Electr. Syst. **49**(3), 1839–1868 (2013)
8. Skolnik, M.: Introduction to Radar Systems, 3rd edn, pp. 392–393. Publishing House of Electronics Industry, Beijing (2007). (Trans. by, Q.S. Zhuo)
9. Howland, P.E., Clutterbuck, C.F.: Estimation of target altitude in HF surface wave radar. In: Seventh International Conference on Hf Radio Systems and Techniques, pp. 296–300. IET (1997)
10. Zhang, S., Jin, Y.G., Yu, C.J., et al.: HPEKF algorithm of target altitude estimation initializing in HF surface wave radar. J. Harbin Inst. Technol. **39**(5), 725–729 (2007)
11. Gai, M.J., Xiao, Y., You, H., et al.: An approach to tracking a 3D-target with 2D-radar. In: IEEE International Radar Conference, pp. 763–768. IEEE (2005)
12. Guo, R.J., Yuan, Y.S., Quan, T.F.: Study of anti-weak aerial target tracking for high frequency surface wave radar. J. Acta Electron. Sin. **16**(2), 1586–1589 (2005)
13. Rotheram, S.: Ground-wave propagation. Part 1: theory for short distances. IEE Proc. F – Commun. Radar Signal Process. **128**(5), 275–284 (1981)
14. Rotheram, S.: Ground-wave propagation. Part 2: theory for medium and long distances and reference propagation curves. IEE Proc. **128**(5), 285–295 (1981)